CCR6-deficient mice have impaired leukocyte homeostasis and altered contact hypersensitivity and delayed-type hypersensitivity responses

Rosa Varona, … , Carlos Martínez-A., Gabriel Márquez

Rapid Publication

CCR6 expression in dendritic, T, and B cells suggests that this β-chemokine receptor may regulate the migration and recruitment of antigen-presenting and immunocompetent cells during inflammatory and immunological responses. Here we demonstrate that $CCR6^{-/-}$ mice have underdeveloped Peyer's patches, in which the myeloid CD11b$^-$ CD11c$^+$ dendritic-cell subset is not present in the subepithelial dome. $CCR6^{-/-}$ mice also have increased numbers in T-cell subpopulations within the intestinal mucosa. In 2,4-dinitrofluorobenzene–induced contact hypersensitivity (CHS) studies, $CCR6^{-/-}$ mice developed more severe and more persistent inflammation than wild-type (WT) animals. Conversely, in a delayed-type hypersensitivity (DTH) model induced with allogeneic splenocytes, $CCR6^{-/-}$ mice developed no inflammatory response. The altered responses seen in the CHS and DTH assays suggest the existence of a defect in the activation and/or migration of the CD4$^+$ T-cell subsets that downregulate or elicit the inflammation response, respectively. These findings underscore the role of CCR6 in cutaneous and intestinal immunity and the utility of $CCR6^{-/-}$ mice as a model to study pathologies in these tissues.

Find the latest version:

https://jci.me/11297/pdf

CCR6-deficient mice have impaired leukocyte homeostasis and altered contact hypersensitivity and delayed-type hypersensitivity responses

Rosa Varona, Ricardo Villares, Laura Carramolino, Íñigo Goya, Ángel Zaballos, Julio Gutiérrez, Miguel Torres, Carlos Martínez-A., and Gabriel Márquez

Departamento de Inmunología y Oncología, Centro Nacional de Biotecnología,
Consejo Superior de Investigaciones Científicas, Universidad Autónoma de Madrid, Cantoblanco, Madrid, Spain

Address correspondence to: Gabriel Márquez, Departamento de Inmunología y Oncología,
Centro Nacional de Biotecnología, Universidad Autónoma de Madrid, Cantoblanco, E-28049 Madrid, Spain.
Phone: 34-91-585-4856; Fax: 34-91-372-0493; E-mail: gmarquez@cnb.uam.es.

CCR6 expression in dendritic, T, and B cells suggests that this β-chemokine receptor may regulate the migration and recruitment of antigen-presenting and immunocompetent cells during inflammatory and immunological responses. Here we demonstrate that $CCR6^{-/-}$ mice have underdeveloped Peyer's patches, in which the myeloid CD11b$^+$ CD11c$^+$ dendritic-cell subset is not present in the subepithelial dome. $CCR6^{-/-}$ mice also have increased numbers in T-cell subpopulations within the intestinal mucosa. In 2,4-dinitrofluorobenzene–induced contact hypersensitivity (CHS) studies, $CCR6^{-/-}$ mice developed more severe and more persistent inflammation than wild-type (WT) animals. Conversely, in a delayed-type hypersensitivity (DTH) model induced with allogeneic splenocytes, $CCR6^{-/-}$ mice developed no inflammatory response. The altered responses seen in the CHS and DTH assays suggest the existence of a defect in the activation and/or migration of the CD4$^+$ T-cell subsets that downregulate or elicit the inflammation response, respectively. These findings underscore the role of CCR6 in cutaneous and intestinal immunity and the utility of $CCR6^{-/-}$ mice as a model to study pathologies in these tissues.

Introduction

Leukocyte traffic is the hallmark of the immune response. Controlled cell movements allow the precise interactions necessary to bring different leukocytes into physical contact. The possibility of rare T and B lymphocytes encountering their specific antigen is maximized by their recirculation through secondary lymphoid organs, in which antigens are displayed to them by antigen-presenting cells. Of these, dendritic cells (DCs) are an important heterogeneous population of antigen-presenting cells that can induce, sustain, and regulate immune responses (1). Once activated, effector T cells are able to migrate to tissues in which pathogens have been detected. Eventually, memory T cells constitute a surveillance system that ensures tissue protection in case of a new antigen challenge. In recent years, several reports have pointed to chemokines as important factors in the regulation of leukocyte trafficking, both in physiological and pathological situations (2–7).

CCR6 is a β-chemokine–specific receptor for CCL20 (MIP-3α/LARC/Exodus) (8–13). In addition to having only one highly specific ligand, other features make CCR6 an interesting receptor. Human (h)CCR6 is expressed in immature DCs derived in vitro from CD34$^+$ precursors and is downregulated as DCs mature (14, 15); it is also expressed in memory T cells, CLA$^+$ cells, and B cells (16). Similar CCR6 expression patterns have been reported in the mouse, in which CCR6 is expressed in the myeloid but not in the lymphoid DC subpopulation (17, 18), B cells and CD4$^+$ T cells (17).

CCL20 is known to interact only with CCR6 in both the human and murine systems. Human CCL20 triggers adhesion of memory CD4$^+$ T cells to ICAM-1 (19) and is expressed in epithelial crypts of inflamed tonsils (14), epithelial cells from appendix (20), as well as keratinocytes and venular endothelial cells from non-pathological skin (21) and psoriatic skin (22, 23). Murine CCL20 (mCCL20) was also reported to be expressed in epithelial cells from intestinal tissue (20); interestingly, in Peyer's patches (PPs) mCCL20 is expressed only by the follicle-associated epithelium (FAE) overlying the subepithelial dome (SED), where CCR6-expressing cells accumulate (18).

Taken together, these data suggest a role for CCR6 and its ligand as regulators of the migration and

recruitment of antigen-presenting and immunocompetent cells during inflammatory and immunological responses. Indeed, while this manuscript was in preparation, Cook et al. reported data on *CCR6*$^{-/-}$ mice showing that this β-chemokine receptor is a regulator of the humoral immunity and lymphocyte homeostasis in the intestinal mucosa (24). We have also generated *CCR6*$^{-/-}$ mice to investigate the CCR6 role in vivo. Analysis of these mice revealed defects in leukocyte homing to the intestinal mucosa as evidenced by their underdeveloped PPs, in which clear alterations in the positioning of myeloid CD11b$^+$ CD11c$^+$ DCs were observed. These animals also showed increased numbers of intraepithelial lymphocyte (IEL) subpopulations. The altered responses of *CCR6*$^{-/-}$ mice in contact hypersensitivity (CHS) and delayed-type hypersensitivity (DTH) models of inflammation suggest additional roles for CCR6 in the activation and/or migration of CD4$^+$ T-cell subsets.

Methods

Gene targeting. Gene targeting was performed according to established methods (25). A 7-kb *Bam*HI DNA fragment containing the CCR6 gene was subcloned from a phage P$_1$ mouse genomic library (Genome Systems Inc., St. Louis, Missouri, USA), as described (17). A 2.7-kb *Pst*I-*Eco*RI and a 2.7-kb *Sma*I-*Xba*I fragment from the CCR6 gene 5′ and 3′ regions, respectively, were then subcloned at either end of a neomycin resistance gene, under the control of the phosphoglycerate kinase promoter. The herpes simplex thymidine kinase gene was fused at the 5′ end of the cloned CCR6 sequences in the replacement targeting construct, which was then linearized by *Not*I digestion and electroporated into the 129 SvJ R1 (26) embryonic stem (ES) cell line. Ganciclovir and G418-resistant clones were selected, and 10 μg of genomic DNA from each clone was *Bam*HI digested, subjected to electrophoresis, and blotted onto Hybond-N$^+$ membranes (Amersham Pharmacia Biotech, Piscataway, New Jersey, USA). High-stringency hybridizations with CCR6-specific ^{32}P-labeled probes were performed in Rapid-Hyb buffer (Amersham Pharmacia Biotech). Probe A was derived from a region upstream of the 5′ homology region (Figure 1).

Three independent correctly targeted ES clones were used to produce chimeric mice by aggregation with CD1 morulae, which were then transferred to pseudopregnant CD1 females, as described elsewhere (25). Chimeric males were bred to C57BL/6, and the offspring genotype was analyzed by Southern blotting and PCR with specific primers. Transcription of the *CCR6* gene was analyzed by Northern blotting, using a DNA fragment internal to the *CCR6* coding sequence as probe. Age- and sex-matched, 8- to 16-week-old 129 SvJ × C57BL/6 F$_3$ or F$_4$ *CCR6*$^{-/-}$ animals were used throughout this study; 129 SvJ × C57BL/6 F$_3$ or F$_4$ *CCR6*$^{+/+}$ mice were used as controls.

Cell preparations. Mice were sacrificed by cervical dislocation. Inguinal, axillary, and brachial (IAB) lymph nodes (LNs), mesenteric LNs, PPs, spleen, and small intestine were collected. The organs were gently disrupted in RPMI with 10% FCS and filtered through nylon mesh to remove aggregates. Splenocytes were depleted of erythrocytes by lysis with 0.83% ammonium chloride.

For IEL preparations, small intestine, free of fat, PPs, and fecal content, was cut longitudinally. After two washes with 30 ml of Ca^{2+}- and Mg^{2+}-free HBSS (CMF-HBSS) containing 2% FCS and 10 mM HEPES, pH 7.2, intestines were rinsed quickly with cold CMF-HBSS containing 5% FCS and 5 mM EDTA. The samples were then incubated (37°C, 30 minutes, with stirring) in CMF-HBSS with 10% FCS and 5 mM EDTA. Supernatants were then collected and intestines vortexed for 10 seconds in 40 ml of the same solution. Supernatants were pooled and passed through a prewashed 10-ml nylon wool column. The recovered cells were separated in a discontinuous Percoll (Amersham Pharmacia Biotech) gradient, and IEL were recovered from the interface between the 67% and 44% layers.
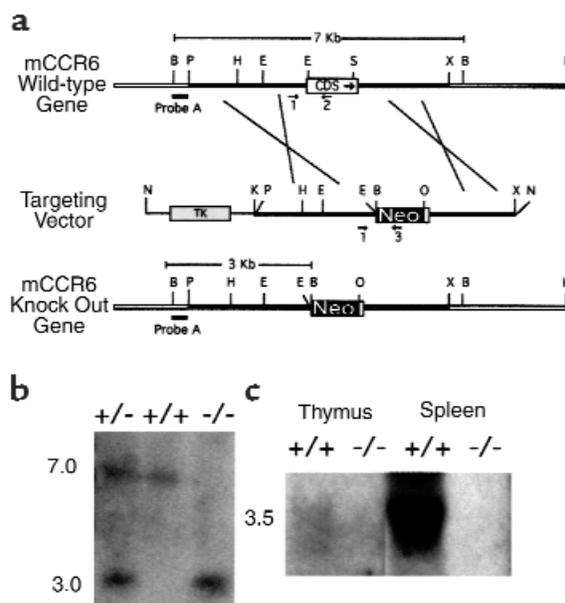

Figure 1
Targeted disruption of the CCR6 gene. (**a**) Targeting strategy. *CCR6* WT locus with partial restriction map. The coding sequence (CDS), neomycin resistance gene (*Neo*), and thymidine kinase gene (*TK*) are shown as open, filled, and shaded boxes, respectively. A thick filled bar shows probe A, used in Southern blot analysis for screening genomic DNA. Arrows mark the position and direction of synthesis of oligonucleotides used in PCR genotyping. B, *Bam*HI; P, *Pst*I; H, *Hind*III; E, *Eco*RI; S, *Sma*I; X, *Xba*I; N, *Not*I; K, *Kpn*I; O, *Xho*I. (**b**) Representative Southern blot analysis of *Bam*HI-digested tail DNA from WT (+/+), heterozygous (+/–), and homozygous (–/–) *CCR6* mice using probe A. Band sizes in kilobases for the WT and knockout alleles are indicated on the left. (**c**) Representative Northern blot analysis of the *CCR6* mRNA expression in thymus and spleen from *CCR6* WT (+/+) and knockout (–/–) animals. The size of the CCR6 transcript in kilobases is indicated on the left.
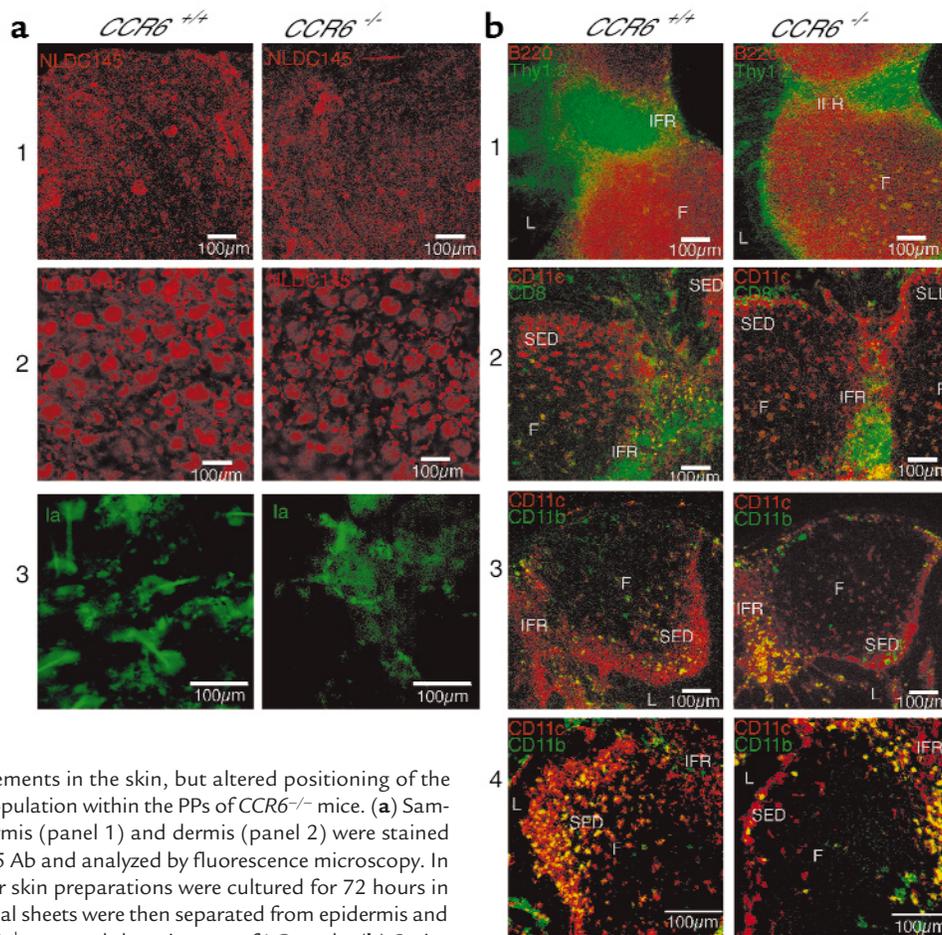
Figure 2

Similar LC complements in the skin, but altered positioning of the myeloid DC subpopulation within the PPs of *CCR6*^{−/−} mice. (**a**) Samples of skin epidermis (panel 1) and dermis (panel 2) were stained with the NLDC145 Ab and analyzed by fluorescence microscopy. In panel 3, dorsal ear skin preparations were cultured for 72 hours in RPMI-1640. Dermal sheets were then separated from epidermis and stained with anti-Ia[b] to reveal the existence of LC cords. (**b**) Staining of WT (*CCR6*^{+/+}) and knockout (*CCR6*^{−/−}) mouse PPs with anti-B220 (red) and anti-Thy1.2 (green) reveals B cells in follicles (F) and T cells in the IFR. For orientation, lumen (L) position is indicated. In panel 2, staining with anti-CD11c (red) and anti-CD8α (green) localizes lymphoid DC mainly in the IFR. In panels 3 and 4, staining with anti-CD11c (red) and anti-CD11b (green) shows a defect in the positioning of myeloid DC in *CCR6*^{−/−} mice, where they are located mainly in the IFR and not in SED. Scale bars = 100 μm.

Flow-cytometry studies. The following FITC-, phycoerythrin- (PE-), Tri-color– (TC-), or SpectralRed- (SPRD-) conjugated mAb's from PharMingen (San Diego, California, USA) were used in this work: anti-CD69 (H1.2F3), anti-CD3 (145-2C11), anti-CD4 (H129.19), anti-CD8 (53-6.7), anti-B220 (RA3-6B2), anti-CD45 (30F11), anti-Thy1.2 (53-2.1), anti–TCR-αβ (H57-597), and anti–TCR-γδ (GL3). Cell staining and flow cytometry were performed in an EPICS XL flow cytometer (Coulter Electronics Ltd., Hialeah, Florida, USA), according to standard protocols.

Skin explants. Ear skin was split into dorsal and ventral portions, and epidermal and dermal sheets were prepared from dorsal portions, before (fresh skin) or after 72-hour culture in complete RPMI-1640 media (skin explants), as described (27).

Immunohistochemistry. Epidermal and dermal sheets from ear (fresh skin or skin explants) were fixed in acetone for 20 minutes. They were then sequentially incubated with rat anti-mouse NLDC145 (LABGEN, Frankfurt, Germany), followed by biotinylated goat anti-rat IgG (H+L) (Southern Biotechnology Associates, Birmingham, Alabama, USA), and streptavidin-Cy3 (Amersham Pharmacia Biotech), or anti-Ia[b] (AF.6-120.1; PharMingen). All incubations were carried out in the presence of 5% normal goat serum (NGS) and 1% BSA in PBS; an avidin/biotin blocking kit (Vector Laboratories, Burlingame, California, USA) was also used after incubation with the primary Ab. Density of Langerhans' cell (LC) population within dermal sheets was determined by direct counts of labeled cells in a defined area of an ocular grid, magnifying ×100. Ten random fields on sheets were counted for each animal.

Frozen PPs were cut in 10-μm sections, fixed in cold acetone for 10 minutes, and stored at –80°C. PP sections were blocked (30 minutes) with 20% NGS, 1% BSA in PBS, followed when necessary by incubation with the avidin/biotin blocking kit. All Ab incubations were performed in 1% NGS and 1% BSA in PBS. The following Ab's from PharMingen were used: biotinylated anti-CD8, anti-CD11c (N418), anti-CD11b (M1/70), and anti-B220-PE. In addition, anti-Thy1.2-
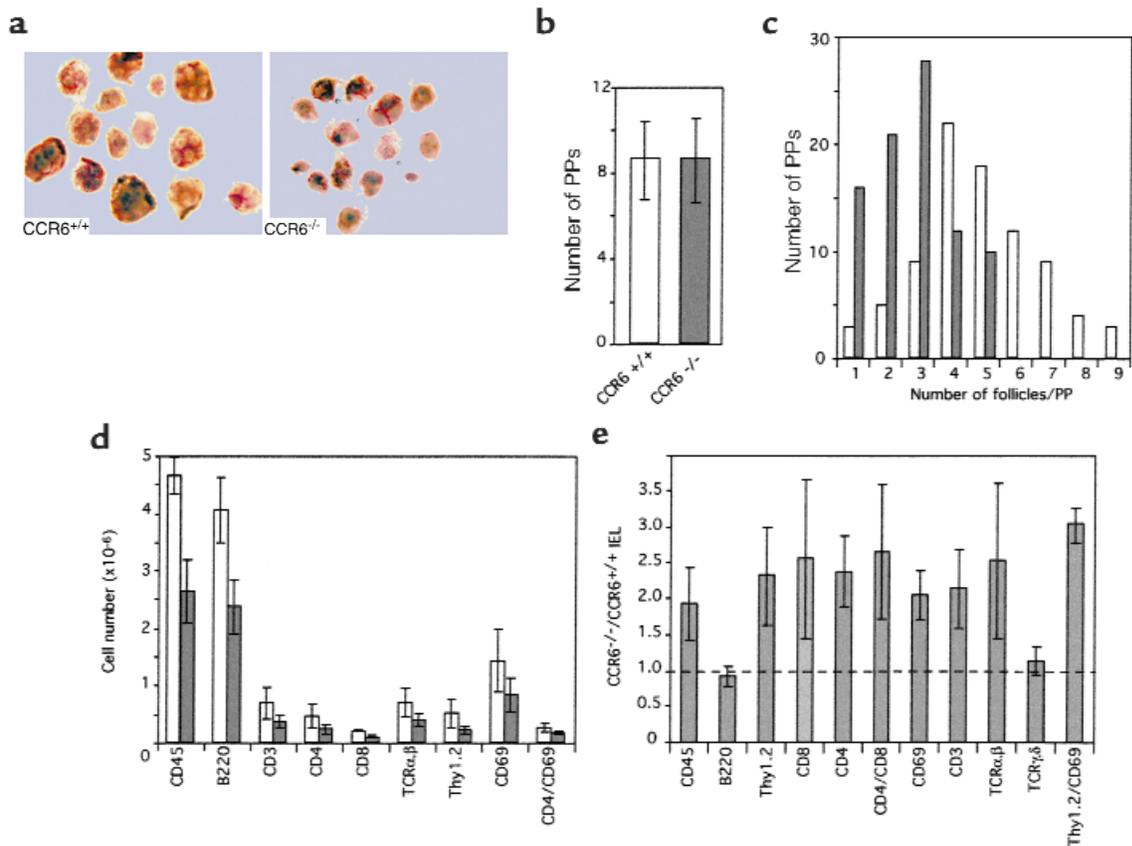
Figure 3

CCR6$^{-/-}$ mice have underdeveloped PPs and impaired lymphocyte homeostasis in the intestinal mucosa. (**a**) Low-magnification micrography of dissected PPs from 4-month-old WT (*CCR6$^{+/+}$*) and *CCR6$^{-/-}$* mice showing the different level of development of these lymphoid organs. (**b**) The number of PPs is similar in WT (*CCR6$^{+/+}$*) and *CCR6$^{-/-}$* mice. Data shown correspond to the average number found in ten animals of each genotype. (**c**) The number of developed follicles per patch and the number of PPs with a given developmental state differ in *CCR6$^{-/-}$* mice (filled bars) from those of WT animals (open bars). Accumulated data are presented from ten animals per group. (**d**) Flow-cytometry analysis of lymphocyte subsets in PPs of WT (open bars) and *CCR6$^{-/-}$* mice (filled bars). (**e**) The cell numbers in IEL subpopulations are increased in *CCR6$^{-/-}$* mice (*n* = 2–3 pooled animals of each genotype in each experiment). Data shown in **d** and **e** correspond to the mean and SE from five independent experiments.

FITC (Becton Dickinson, Oxford, United Kingdom), streptavidin-Cy2, and streptavidin-Cy3 (Amersham Pharmacia Biotech) were used.

Subcutaneous immunization. Animals (8–10 weeks old) were immunized subcutaneously in the dorsum with 30 μg dinitrophenyl–keyhole limpet hemocyanin (DNP-KLH) in CFA, and boosted twice with 30 μg of DNP-KLH in incomplete Freund's adjuvant at days 10 and 28 after immunization. DNP-KLH–specific serum Ab titers were determined by serial dilution of serum in DNP-KLH–coated 96-well plates. Ab's bound to plates were developed with peroxidase-conjugated isotype-specific Ab's (Southern Biotechnology Associates) and diaminobenzidine (Sigma Chemical Co., St. Louis, Missouri, USA).

Contact hypersensitivity. The mouse ear-swelling test has been described elsewhere (28). Briefly, mice were sensitized topically by applying 25 μl of 0.5% 2,4-dinitrofluorobenzene (DNFB; Sigma Chemical Co.) solution in acetone/olive oil (4:1) to the shaved abdomen. Five days later, 20 μl of 0.2% DNFB in the same vehicle was applied to the

right ears, and vehicle alone to the left ears. Ear thickness was measured with a dial thickness gauge (Mitutoyo Corp., Kawasaki, Japan), and ear swelling was estimated by subtracting the prechallenge from the postchallenge value, and by further subtracting any swelling detected in the vehicle-challenged contralateral ear.

Delayed-type hypersensitivity. Mice were sensitized by intravenous injection of 10^6 BALB/c splenocytes, and challenged on day 5 with 13 × 10^6 BALB/c splenocytes (50 μl PBS) in the right footpads. Control left footpads received 50 μl PBS. Right footpad swelling was calculated on different days by subtracting the prechallenge value and any swelling measured in left footpads from the postchallenge value.

For adoptive transfer experiments, cell suspensions from LNs of BALB/c splenocyte-sensitized or untreated control animals were depleted of B220$^+$ and CD8$^+$ cells by incubation with rat anti-mouse B220-FITC and CD8-FITC, followed by separation in MACS columns with paramagnetic anti-FITC microbeads (Miltenyi Biotech, Auburn, California, USA). Eluted CD4$^+$ T cell–enriched

Figure 4

Serum concentrations of antigen-specific immunoglobulins in animals immunized with DNP-KLH. *CCR6*$^{-/-}$ (*n* = 7; circles) and *CCR6*$^{+/+}$ (*n* = 7; squares) mice were immunized subcutaneously with 30 µg of DNP-KLH in CFA and boosted twice with 30 µg of DNP-KLH in IFA at days 10 and 28 postimmunization. Mice were bled from the retro-orbital plexus at days 7 and 14, then every 21 days, and serum concentration of DNP-KLH–specific Ig isotypes were determined using ELISA. Individual data from the 10^{-3} dilution and the mean value for each group are presented. Two-tailed *t*-test value for the IgG2b data at day 35 is *P* = 0.0032; *P* > 0.05 for the rest.


preparations were injected into the tail vein of recipient mice (2 × 10^7 cells/mouse). After 16 hours, mice were challenged by injecting 13 × 10^6 BALB/c splenocytes (without red blood cells) into the right footpads, and swelling was monitored throughout the following days.

In vitro antigen-presentation assays. In vitro lymphocyte proliferation to 2,4-dinitrobenzenesulphonic acid (DNBS), the water-soluble analogue of DNFB, was carried out as described (29). Briefly, IAB LNs from *CCR6*$^{-/-}$ and wild-type (WT) littermate control mice, untreated or sensitized with DNFB in the abdomen 5 days before, were collected and pooled. Mesenteric LNs were also collected. LN cells were then cultured alone or in the presence of DNBS (50 µg/ml). Polyclonal activation of lymphocytes was performed by incubating LN cells with 5 µg/ml of Con A (Sigma Chemical Co.) for 48 hours. All cultures were then pulsed with 1 µCi/well of ^{3}H-thymidine for 18 hours.

Allogeneic mixed lymphocyte reactions (MLR) were performed as described (30). Stimulating cells were BALB/c splenocytes, inactivated with 50 µg/ml of mitomycin C (37°C, 20 minutes). Responding cells were WT or *CCR6*$^{-/-}$ lymphocyte pools from IAB LNs. Stimulating and responding cells were cocultured (37°C, 72 hours) at different ratios, then pulsed with 1 µCi/well of ^{3}H-thymidine for 24 hours.

Results and Discussion

Generation of CCR6$^{-/-}$ *mice*. The mouse *CCR6* gene was replaced by homologous recombination, using the targeting strategy shown in Figure 1a. This procedure deleted most of the exon containing the CCR6 coding sequence, leaving only the nucleotides encoding the 25 COOH-terminal amino acids of the receptor. Southern blot analysis of ES clones surviving selection in culture allowed the detection of those that underwent homologous recombination. Morulae aggregations were carried out with three targeted ES clones to generate chimeric mice, selecting two independent animals that transmitted the disrupted *CCR6* allele through the germline. Chimeras were mated with C57BL/6 mice, and heterozygous animals from F$_1$ and subsequent offspring were backcrossed for three to four generations with WT C57BL/6 mice. Southern blot analysis of tail DNA confirmed the CCR6 coding sequence deletion (Figure 1b). Northern blot analysis also confirmed the lack of CCR6 mRNA (Figure 1c).
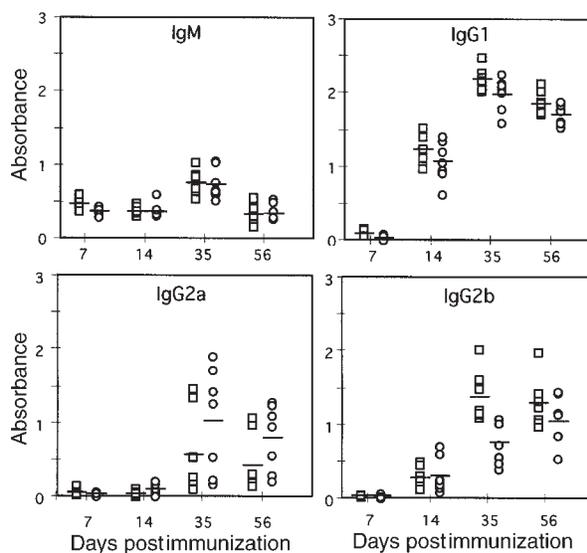
Mice maintained under barrier isolation were healthy, and bred according to Mendelian inheritance patterns. No phenotypic differences were detected between the two *CCR6*$^{-/-}$ mouse lines generated. Several organs, such as spleen, thymus, and LNs, and their resident leukocyte populations were examined, and no differences were found between *CCR6*$^{-/-}$ mice and the corresponding WT animals. The hematological and bone marrow profiles of WT and *CCR6*$^{-/-}$ mice were also similar (results not shown).

CCR6$^{-/-}$ *mouse skin has a normal LC complement, able to migrate from the epidermis into the dermis*. CCR6 is selectively expressed among the different DC subpopulations. In humans, CCR6 is expressed mainly in immature DCs (14, 15). Furthermore, the CCR6 ligand, CCL20, was proposed to have a role in regulating the constitutive trafficking of epidermal LCs (21), a fact that has not been confirmed by others (22).

We addressed these issues by searching for differences in the number of LCs between WT and *CCR6*$^{-/-}$ mice. The LC population in epidermis from the ear (Figure 2a, panel 1) or abdominal skin (not shown) was analyzed using immunohistochemistry. Surprisingly, no differences were detected in the LC population between WT and *CCR6*$^{-/-}$ mice; this was further confirmed when cells in ten random microscopic fields were counted at a magnification of ×100 (not shown). Similar results were obtained when dermis was analyzed (Figure 2a, panel 2). Local inflammatory responses induce LC to migrate from the epidermis into the dermis, where they form cords in dermal lymphatics, after which they migrate out of the skin. Skin explants that allow the in vitro reproduction of this LC migration (27) were performed, and the results showed that LC from *CCR6*$^{-/-}$ mice migrated from the epidermis to the dermis, where they formed the characteristic cell cords (Figure 2a, panel 3). Taken together, these results show that LCs without a functional CCR6 receptor are equally able to reach the skin and egress from this tissue after being stimulated to

migrate and suggest that the CCL20/CCR6 pair is not an essential component in the control of physiological LC trafficking to the skin. Nevertheless, the reported CCL20 and CCR6 upregulation in the skin of psoriatic patients (22, 23) indicates that these proteins might play an important role in skin pathologies.

CCR6-deficient mice have underdeveloped PPs with altered positioning of the myeloid DC subpopulation and impaired lymphocyte homeostasis in intestinal mucosa. In the mouse, CCR6 is expressed by myeloid spleen DCs but not by the lymphoid DC subset (17). A recent report (18) on the localization of distinct DC subsets within the PP showed that mCCL20 mRNA is expressed mainly in the FAE. Correspondingly, CCR6 mRNA is strongly expressed beneath the FAE, within the SED; in addition, mCCR6 is also detected under the SED, where follicle B cells are located (18). Consistent with these results, CD11b+ CD11c+ CD8α– myeloid CCR6-expressing DCs are located in the SED region and absent from the interfollicular region (IFR), whereas lymphoid CD11b– CD11c+ CD8α+ DC, which do not express CCR6, are located in the IFR (18).

We looked for possible alterations in the localization of these DC subpopulations in the *CCR6–/–* mice.

Frozen PP sections were stained with different markers, and the results showed normal B- and T-cell distribution in the follicles and IFR, respectively (Figure 2b, panel 1). Consistent with the results reported by Iwasaki and Kelsall (18), CD11c+ CD8α+ lymphoid DCs were located in the IFR (Figure 2b, panel 2). The CD11b+ CD11c+ myeloid DCs showed altered distribution in *CCR6–/–* mice (Figure 2b, panels 3 and 4), however, and were present mainly in the IFR and not in the SED, as was the case in WT animals.

These were not the only alterations detected in PPs from *CCR6–/–* animals. Regardless of the age of the animals examined, PPs from *CCR6–/–* mice were systematically smaller, showing a lower number of developed follicles than those from WT animals; nonetheless, the number of PPs along the small intestine was similar in both animal groups. Results from a representative analysis are shown (Figure 3, a–c). These observations were further substantiated by flow cytometry analysis of PPs and small intestine lymphocyte subsets. No alterations were found in the relative proportions of the different lymphocyte subsets analyzed in PPs from *CCR6–/–* mice, but, consistent with their reduced size, our results revealed a twofold decrease in the number
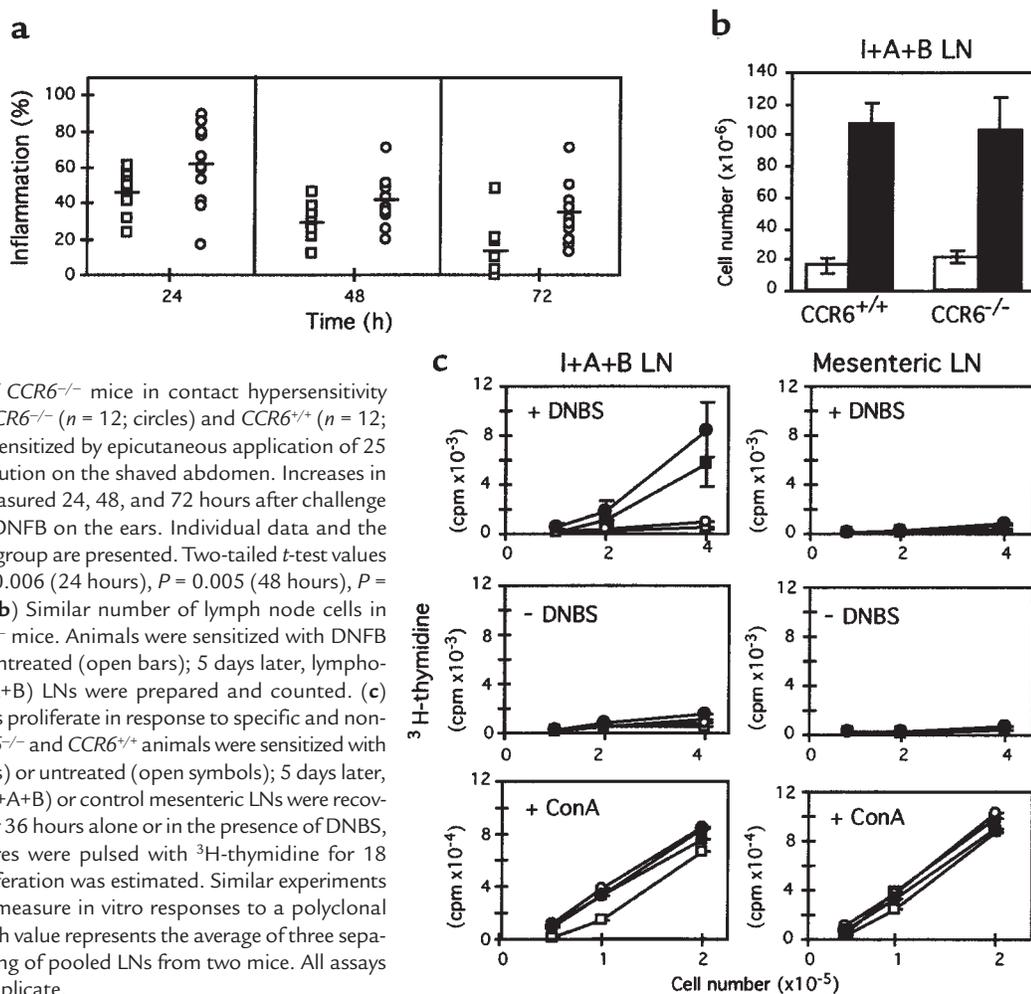
Figure 5

Altered response of *CCR6–/–* mice in contact hypersensitivity inflammation. (**a**) *CCR6–/–* (n = 12; circles) and *CCR6+/+* (n = 12; squares) mice were sensitized by epicutaneous application of 25 µl of 0.5% DNFB solution on the shaved abdomen. Increases in ear swelling were measured 24, 48, and 72 hours after challenge with 20 µl of 0.2% DNFB on the ears. Individual data and the mean value for each group are presented. Two-tailed *t*-test values for DNFB data: *P* = 0.006 (24 hours), *P* = 0.005 (48 hours), *P* = 0.002 (72 hours). (**b**) Similar number of lymph node cells in *CCR6+/+* and *CCR6–/–* mice. Animals were sensitized with DNFB (filled bars) or left untreated (open bars); 5 days later, lymphocytes from IAB (I+A+B) LNs were prepared and counted. (**c**) *CCR6–/–* lymphocytes proliferate in response to specific and nonspecific stimuli. *CCR6–/–* and *CCR6+/+* animals were sensitized with DNFB (filled symbols) or untreated (open symbols); 5 days later, cells from draining (I+A+B) or control mesenteric LNs were recovered and cultured for 36 hours alone or in the presence of DNBS, as indicated. Cultures were pulsed with ^{3}H-thymidine for 18 hours, and cell proliferation was estimated. Similar experiments were performed to measure in vitro responses to a polyclonal stimulus, Con A. Each value represents the average of three separate groups, consisting of pooled LNs from two mice. All assays were performed in triplicate.

Figure 6

CCR6−/− mice have a markedly diminished DTH response to allogeneic BALB/c splenocytes. (**a**) *CCR6−/−* (*n* = 10; circles) and *CCR6+/+* (*n* = 11; squares) animals were sensitized by intravenous injection of 10^6 BALB/c splenocytes. Five days later, mice were challenged by injecting 13×10^6 BALB/c splenocytes into their right footpads, and swelling was measured 24 hours later. Individual data and the mean value for each group are presented. The two-tailed *t*-test value for these data was *P* = 0.000016. (**b**) In vitro MLR to allogeneic BALB/c splenocytes. Lymphocytes were prepared from IAB LNs from *CCR6+/+* (filled squares) and *CCR6−/−* mice (filled circles) and cultured in 96-well plates (2×10^5 cells/well) with increasing amounts of stimulator allogeneic BALB/c splenocytes. After 72 hours, cultures were pulsed with ^{3}H-thymidine for 24 hours and cell proliferation was estimated. Background proliferation is also shown (open symbols). Each point represents the average value of two separate groups, each consisting of pooled LNs from two mice. Assays were performed in triplicate. (**c**) Adoptive transfer of sensitized *CCR6+/+* CD4+ T cells to *CCR6−/−* mice restores their ability to produce a DTH response. Unsensitized *CCR6+/+* and *CCR6−/−* mice were adoptively transferred with 2×10^7 CD4+ T cell–enriched preparations purified from sensitized *CCR6+/+* and *CCR6−/−* donors, as indicated. T cells from *CCR6−/−* IAB LNs were also allowed to proliferate in an in vitro MLR assay with BALB/c splenocytes before being injected to *CCR6−/−* hosts (++). After 16 hours, animals were challenged with 13×10^6 BALB/c splenocytes in footpads, and swelling was measured 24 hours later.

of total leukocytes estimated as CD45+ cells in PPs from mutant mice (Figure 3d). B220+, CD3+, CD4+, CD8+, TCR-αβ, and CD69+ cells were all reduced approximately twofold in *CCR6−/−* mice. Conversely, when IEL subpopulations were examined, the results (Figure 3e) showed that CCR6 mutant mice had an overall twofold increase in total lymphocytes, with greater increases in the CD4+ CD8+ double-positive, CD4+, CD8+, TCR-αβ, and especially the Thy1.2+ CD69+ cell subsets. No differences were detected in B cells, estimated as B220+ cells, nor in TCR-γδ cells.

Mucosal membranes of the intestinal tissue are constantly exposed to antigens. The organized mucosa-associated lymphoid tissues function as inductive sites. M cells present in the FAE capture antigens and internalize them to the underlying lymphoid tissue, where they can be processed and presented by macrophages, DCs, and B cells, thus generating the immune response. The altered position of the CD11b+ CD11c+ myeloid DCs outside the SED in *CCR6−/−* mice may be a factor contributing to the impaired PP development in these mice, reflected by both diminished cellularity and number of developed follicles. Exposure to intestinal flora is essential for the complete development of the gut-associated lymphoid tissue (31). The alterations detected in myeloid DCs in *CCR6−/−* mouse PPs may thus provoke defects in the presentation mechanism of flora or other antigens, impairing PP development. In addition, B lymphocytes play an organogenic role in mucosal immunity, as demonstrated by the impaired development of PPs, FAE, and M cells in mice lacking B cells (32). B-cell numbers are reduced in PPs from *CCR6−/−* mice (Figure 3), but there is no definitive proof as to whether this is a cause or an effect of PP underdevelopment. Anyway, CCR6 is normally
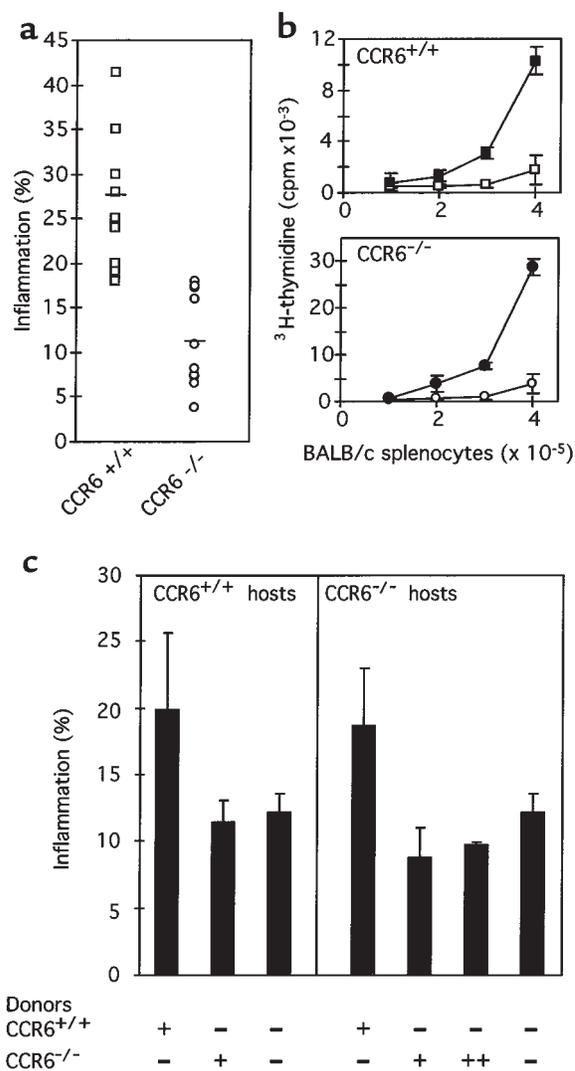
expressed in both human and mouse B cells, thus making possible a hypothetical role for this chemokine receptor in PP organogenesis. Gene disruption of lymphotoxins or their cognate receptors has also been reported to affect PP development (33); the expression level of these genes in *CCR6−/−* mice will be the subject of future investigations.

While this manuscript was in preparation, Cook et al. reported similar results on the altered positioning of myeloid DCs within PPs and increases in the IEL subpopulations of CCR6 mutant mice (24). There is nonetheless discrepancy with our results in PPs, which are normal in their *CCR6−/−* mice. The distinct genetic backgrounds of the animals used in the two studies are unlikely to be responsible for the difference, since this PP phenotype was already detected in our F_1 mice. It is possible, however, that differences in the animal diets, in which the presence of sensitizing antigens may amplify differences in PP development between WT and *CCR6−/−* mice, account for this discrepancy in results. In addition, different bacterial loads in mice could also explain the differences in PP development.

Humoral response to subcutaneous immunization. To analyze the possibility of a defective systemic humoral response in *CCR6*$^{-/-}$ mice, animals received DNP-KLH subcutaneously, and their serum DNP-KLH–specific Ig levels were determined on different days. No differences in antigen-specific IgM and IgG1 were detected between WT and *CCR6*$^{-/-}$ animals (Figure 4). In contrast, some minor differences in DNP-KLH–specific IgG2b levels, lower in *CCR6*$^{-/-}$ mice, were detected (P = 0.0032; Figure 4). Antigen-specific IgG2a levels were higher in the *CCR6*$^{-/-}$ animals, but these differences were not statistically significant (P > 0.05; Figure 4). Immunoglobulin class-switch recombination occurs in mature B cells after contact with antigen. Since B cells express CCR6, it is conceivable that *CCR6*$^{-/-}$ B cells are affected in this process, giving rise to the differences observed. In addition to antigen contact, it is thought that concomitant cytokine signaling controls Ig isotype specificity in class switching (34). It could thus be speculated that altered cytokine levels might contribute to the minor abnormalities detected in the systemic immune response to DNP-KLH in *CCR6*$^{-/-}$ mice.

CHS responses. CHS is a hapten-specific skin inflammation mediated by T cells. Most haptens give rise to an oligoclonal T-cell response consisting mainly of CD8$^+$ effector T cells, whereas CD4$^+$ T cells have a downregulatory role in the CHS response (35, 36). To test the role of CCR6 in CHS, mice were epicutaneously sensitized with DNFB, and then challenged 5 days later by hapten application to ear skin. With DNFB treatment, ear swelling was greater and lasted longer in *CCR6*$^{-/-}$ mice (Figure 5a). We looked for possible differences in lymph node cellularity between WT and *CCR6*$^{-/-}$ mice. Animals were untreated or sensitized with DNFB and, 5 days later, lymphocytes from IAB LNs were prepared and counted. The results showed similar increases in cell numbers in LNs from DNFB-treated WT and *CCR6*$^{-/-}$ mice (Figure 5b), suggesting that similar sensitization responses had taken place in both groups. As predicted, the number of lymphocytes in LNs from untreated animals was clearly lower and similar in both groups (Figure 5b).

We also analyzed the specific proliferative response of lymphocytes from sensitized animals. Cells prepared from LNs were cultured alone or in the presence of DNBS, a water-soluble form of the hapten, and cell proliferation was determined. Again, no differences were detected between WT and *CCR6*$^{-/-}$ animals (Figure 5c). Lymphocytes from IAB LNs of DNFB-sensitized animals showed a clear proliferative response only in the presence of DNBS; control IAB LN lymphocytes from unsensitized animals and mesenteric LN lymphocytes, with or without DNBS, did not proliferate. Finally, we studied the proliferative response to a polyclonal antigen, Con A. In this case, lymphocytes from all LNs studied were equally able to proliferate in the presence of the antigen (Figure 5c). These results suggest that the afferent branch of the hapten-induced inflammation response functions correctly in *CCR6*$^{-/-}$ mice. In CHS, LC participation does not

appear necessary for T-cell sensitization (37); in any case, as shown above, LC numbers in *CCR6*$^{-/-}$ animals are apparently normal, as it is their ability to migrate into the dermis. Interestingly, the increased and persistent inflammation seen in *CCR6*$^{-/-}$ mice suggests that it is the efferent phase of the CHS response that is defective in these animals. Because CD4$^+$ T cells are responsible for downregulating the DNFB-induced inflammation (35), and these cells express CCR6 (16, 17, 19), suppressor CD4$^+$ T-cell control of the inflammatory process may be impaired in *CCR6*$^{-/-}$ mice.

DTH responses. In contrast to CHS, DTH is elicited by CD4$^+$ T cells with apparent downregulatory effects of CD8$^+$ T cells (36). The results observed in the CHS model prompted us to study the behavior of CD4$^+$ T cells from *CCR6*$^{-/-}$ mice in a DTH model. Control WT and *CCR6*$^{-/-}$ C57BL/6 animals were sensitized by intravenous injection of 10^6 allogeneic BALB/c splenocytes. Five days later, 13×10^6 BALB/c splenocytes were injected into the right footpads, and local inflammation was measured. Results at 24 hours showed that, in comparison with WT mice, *CCR6*$^{-/-}$ mouse footpads developed significantly less inflammation (Figure 6a). Lymphocytes from IAB LNs from WT and *CCR6*$^{-/-}$ mice were prepared, and their specific proliferative response to allogeneic BALB/c splenocytes studied in MLR assays. Lymphocytes from *CCR6*$^{-/-}$ mice showed no proliferative defect (Figure 6b).

These results suggested that CD4$^+$ T cells from *CCR6*$^{-/-}$ mice were unable to elicit the efferent phase of the DTH response. To address this question, similar DTH experiments were performed in which CD4$^+$ T cell–enriched preparations purified from the LNs of WT and *CCR6*$^{-/-}$ animals were adoptively transferred to either WT or *CCR6*$^{-/-}$ unsensitized mice 16 hours before footpad challenge. The results (Figure 6c) showed that adoptive transfer of 2×10^7 CD4$^+$ T cells from sensitized WT animals to both WT and *CCR6*$^{-/-}$ mice before challenge caused these animals to develop a similar footpad inflammation. Conversely, when CD4$^+$ T cells from sensitized *CCR6*$^{-/-}$ donors were transferred to WT and *CCR6*$^{-/-}$ mice, the hosts were unable to develop an inflammation response upon injection of BALB/c splenocytes. To be sure that *CCR6*$^{-/-}$ T cells had been in contact with the antigen before being adoptively transferred, purified T cells from *CCR6*$^{-/-}$ IAB LNs were induced to proliferate in an MLR assay with BALB/c splenocytes and then transferred to *CCR6*$^{-/-}$ mice. This procedure did not alter the lack of inflammation response of the hosts (Figure 6c). Taken together, these results strongly suggest that the CD4$^+$ T cells responsible for eliciting the DTH inflammatory response are defective in *CCR6*$^{-/-}$ mice. As commented for the CHS results, this defect may be related to an impaired activation and/or ability to migrate from lymphoid organs to tissues.

In summary, the results reported here show that CCR6 plays a role in the control of leukocyte homeostasis in the intestinal mucosa. The altered positioning of CD11b$^+$ CD11c$^+$ DCs in PPs may contribute to

the differences observed in lymphocyte subsets in *CCR6*⁻/⁻ mice. In addition, migration may be impaired in these *CCR6*⁻/⁻ cells, contributing to the overall defect. The altered responses observed in the CHS and DTH assays suggest a defect in the activation and/or migration of the CD4⁺ T-cell subsets that downregulate or elicit the inflammatory response, respectively, in these inflammation models. Taken together, our data show that CCR6 participates in both homeostatic and inflammatory processes, implying that the in vivo role of its ligand, CCL20, fits within both functional chemokine subfamilies. The finding of nonredundant biological roles for CCR6 underscores the usefulness of *CCR6*⁻/⁻ mice as a model for the study of inflammatory diseases, not only for intestinal but also for cutaneous pathologies such as allergic contact dermatitis, the common clinical form of CHS.

Acknowledgments

1. Banchereau, J., et al. 2000. Immunobiology of dendritic cells. *Annu. Rev. Immunol.* **18**:767–811.
2. Forster, R., et al. 1996. A putative chemokine receptor, BLR1, directs B cell migration to defined lymphoid organs and specific anatomic compartments of the spleen. *Cell.* **87**:1037–1047.
3. Sallusto, F., Lanzavecchia, A., and Mackay, C.R. 1998. Chemokines and chemokine receptors in T-cell priming and Th1/Th2-mediated responses. *Immunol. Today.* **19**:568–574.
4. Sallusto, F., Lenig, D., Forster, R., Lipp, M., and Lanzavecchia, A. 1999. Two subsets of memory T lymphocytes with distinct homing potentials and effector functions. *Nature.* **401**:708–712.
5. Forster, R., et al. 1999. CCR7 coordinates the primary immune response by establishing functional microenvironments in secondary lymphoid organs. *Cell.* **99**:23–33.
6. Cyster, J.G. 1999. Chemokines and cell migration in secondary lymphoid organs. *Science.* **286**:2098–2102.
7. Campbell, J.J., and Butcher, E.C. 2000. Chemokines in tissue-specific and microenvironment-specific lymphocyte homing. *Curr. Opin. Immunol.* **12**:336–341.
8. Baba, M., et al. 1997. Identification of CCR6, the specific receptor for a novel lymphocyte-directed CC chemokine LARC. *J. Biol. Chem.* **272**:14893–14898.
9. Liao, F., et al. 1997. STRL22 is a receptor for the CC chemokine MIP-3α. *Biochem. Biophys. Res. Commun.* **236**:212–217.
10. Power, C.A., et al. 1997. Cloning and characterization of a specific receptor for the novel CC chemokine MIP-3α from lung dendritic cells. *J. Exp. Med.* **186**:825–835.
11. Greaves, D.R., et al. 1997. CCR6, a CC chemokine receptor that interacts with macrophage inflammatory protein 3α and is highly expressed in human dendritic cells. *J. Exp. Med.* **186**:837–844.
12. Rossi, D.L., Vicari, A.P., Franz, B.K., McClanahan, T.K., and Zlotnik, A. 1997. Identification through bioinformatics of two new macrophage proinflammatory human chemokines: MIP-3α and MIP-3β. *J. Immunol.* **158**:1033–1036.
13. Hromas, R., et al. 1997. Cloning and characterization of exodus, a novel β-chemokine. *Blood.* **89**:3315–3322.
14. Dieu, M.C., et al. 1998. Selective recruitment of immature and mature dendritic cells by distinct chemokines expressed in different anatomic sites. *J. Exp. Med.* **188**:373–386.
15. Carramolino, L., et al. 1999. Down-regulation of the β-chemokine receptor CCR6 in dendritic cells mediated by TNF-α and IL-4. *J. Leukoc. Biol.* **66**:837–844.
16. Liao, F., et al. 1999. CC-chemokine receptor 6 is expressed on diverse memory subsets of T cells and determines responsiveness to macrophage inflammatory protein 3α. *J. Immunol.* **162**:186–194.
17. Varona, R., et al. 1998. Molecular cloning, functional characterization and mRNA expression analysis of the murine chemokine receptor CCR6 and its specific ligand MIP-3α. *FEBS Lett.* **440**:188–194.
18. Iwasaki, A., and Kelsall, B.L. 2000. Localization of distinct Peyer's patch dendritic cell subsets and their recruitment by chemokines macrophage inflammatory protein (MIP)-3α, MIP-3β, and secondary lymphoid organ chemokine. *J. Exp. Med.* **191**:1381–1394.
19. Campbell, J.J., et al. 1998. Chemokines and the arrest of lymphocytes rolling under flow conditions. *Science.* **279**:381–384.
20. Tanaka, Y., et al. 1999. Selective expression of liver and activation-regulated chemokine (LARC) in intestinal epithelium in mice and humans. *Eur. J. Immunol.* **29**:633–642.
21. Charbonnier, A.S., et al. 1999. Macrophage inflammatory protein 3α is involved in the constitutive trafficking of epidermal Langerhans cells. *J. Exp. Med.* **190**:1755–1768.
22. Homey, B., et al. 2000. Up-regulation of macrophage inflammatory protein-3α/CCL20 and CC chemokine receptor 6 in psoriasis. *J. Immunol.* **164**:6621–6632.
23. Dieu-Nosjean, M.C., et al. 2000. Macrophage inflammatory protein 3α is expressed at inflamed epithelial surfaces and is the most potent chemokine known in attracting Langerhans cell precursors. *J. Exp. Med.* **192**:705–717.
24. Cook, D.N., et al. 2000. CCR6 mediates dendritic cell localization, lymphocyte homeostasis, and immune responses in mucosal tissue. *Immunity.* **12**:495–503.
25. Torres, M. 1998. The use of embryonic stem cells for the genetic manipulation of the mouse. *Curr. Top. Dev. Biol.* **36**:99–114.
26. Nagy, A., Rossant, J., Nagy, R., Abramow-Newerly, W., and Roder, J.C. 1993. Derivation of completely cell culture-derived mice from early-passage embryonic stem cells. *Proc. Natl. Acad. Sci. USA.* **90**:8424–8428.
27. Larsen, C.P., et al. 1990. Migration and maturation of Langerhans cells in skin transplants and explants. *J. Exp. Med.* **172**:1483–1493.
28. Garrigue, J.L., et al. 1994. Optimization of the mouse ear swelling test for *in vivo* and *in vitro* studies of weak contact sensitizers. *Contact Dermatitis.* **30**:231–237.
29. Phanupak, P., Moorhead, J.W., and Claman, H.N. 1974. Tolerance and contact sensitivity to DNFB in mice. Transfer of tolerance with suppressor T cells. *J. Immunol.* **113**:1230–1236.
30. Coligan, J.E., Kruisbeek, A.M., Margulies, D.H., Shevach, E.M., and Strober, W. 1992. *Current protocols in immunology.* John Wiley & Sons. New York, New York, USA. 1957 pp.
31. Kato, T., and Owen, R.L. 1999. Structure and function of intestinal mucosal epithelium. In *Mucosal immunology.* 2nd edition. P.L. Ogra et al., editors. Academic Press. San Diego, California, USA. 115–132.
32. Golovkina, T.V., Shlomchik, M., Hannum, L., and Chervonsky, A. 1999. Organogenic role of B lymphocytes in mucosal immunity. *Science.* **286**:1965–1968.
33. Debard, N., Sierro, F., and Kraehenbuhl, J.P. 1999. Development of Peyer's patches, follicle-associated epithelium and M cell: lessons from immunodeficient and knockout mice. *Semin. Immunol.* **11**:183–191.
34. Stavnezer, J. 1996. Immunoglobulin class switching. *Curr. Opin. Immunol.* **8**:199–205.
35. Bour, H., et al. 1995. Major histocompatibility complex class I-restricted CD8⁺ T cells and class II-restricted CD4⁺ T cells, respectively, mediate and regulate contact sensitivity to dinitrofluorobenzene. *Eur. J. Immunol.* **25**:3006–3010.
36. Grabbe, S., and Schwarz, T. 1998. Immunoregulatory mechanisms involved in elicitation of allergic contact hypersensitivity. *Immunol. Today.* **19**:37–44.
37. Grabbe, S., Steinbrink, K., Steinert, M., Luger, T.A., and Schwarz, T. 1995. Removal of the majority of epidermal Langerhans cells by topical or systemic steroid application enhances the effector phase of murine contact hypersensitivity. *J. Immunol.* **155**:4207–4217.